

# Quasiparticle Trapping In Three Terminal Ferromagnetic Tunneling Devices

R. Latempa<sup>1,3,\*</sup>, M. Aprili<sup>2,3</sup> and I. Petkovic<sup>2</sup>

1. INFM-Dipartimento di Fisica – Università di Salerno, via S. Allende, 84081 Baronissi (SA) – Italy.
2. Laboratoire de Physique des Solides, Univ. Paris-Sud, CNRS, UMR 8502, F-91405 Orsay Cedex, France.
3. Laboratoire de Physique Quantique, ESPCI, 10 rue Vauquelin 75005 Paris – France.

## Abstract

Hybrid Superconductor/Ferromagnet structures have been investigated recently to address the interplay between ferromagnetism and superconductivity. They also open up new routes for the investigation of out of equilibrium superconductivity. In this paper we show how it is possible for out of equilibrium excitations produced in a superconducting reservoir (S) to be localized in a ferromagnetic trap (F). Specifically, a ferromagnetic nano-volume in good contact with S represents a potential well for the quasiparticles (QPs) at the gap edge. As the superconducting proximity effect is highly suppressed in F, QPs get efficiently trapped and they share their energy with the free electrons in the trap. The electronic temperature  $T_e$  in the trap can be increased by up to 60% from the bath temperature at 320mK as measured by tunneling spectroscopy using a second junction.

PACS numbers: 74.45.+c, 74.50.+r

\*Current address:

Laboratorio MDM-INFM via C.Olivetti, 2 I-20041 Agrate Brianza (MI) Italy

Fax: +39-039-6881175

Phone: +39-039-6037489

e-mail: rossella.latempa@mdm.infm.it

## I. Introduction

Superconductor/Ferromagnet (S/F) hybrid nanostructures open up new routes to study the interplay between superconductivity and ferromagnetism. The main advantage is that unlike in bulk materials, in nanostructures despite the fact that superconducting gap and ferromagnetic exchange energy are not comparable, superconductivity and ferromagnetism do not exclude one another. This is because these two antagonistic ground states influence each other only near the interface. However, nonequilibrium superconductivity in such structures is a new topic. After a superconductor absorbs energy, excess quasiparticles (QPs) with non-thermal distribution are created. Their energy relaxation occurs via two different mechanisms: electron-electron ( $e-e$ ) and electron-phonon ( $e-ph$ ) interactions. The timescale for energy relaxation depends on the respective scattering rates ( $\tau_{ee}^{-1}$  and  $\tau_{e-ph}^{-1}$ ), both of them rapidly increasing with the excitation energy [1]. The Fermi–Dirac energy distribution of QPs is reached on a timescale larger than  $\tau_{ee}$ , while in the limit of strong  $e-ph$  relaxation, QP temperature becomes equal to the lattice temperature [2].

When a superconductor absorbs energy  $E_0$ , within a few picoseconds it goes into a nonequilibrium state, consisting of broken Cooper pairs and high energy phonons with energies close to the cutoff Debye energy [3]. In a fast nanosecond cascade, energy is distributed over an increasing number of QPs and phonons, decaying until it reaches the gap edge. Both excess QPs and phonons have limited lifetimes. QPs may recombine into Cooper pairs, diffuse, get scattered by impurities, or get trapped and frozen, while phonons can get scattered or escape into the substrate. The characteristic timescale of QP recombination into Cooper pairs goes from the  $ns$  until a few  $\mu s$  depending on material parameters [1]. If the superconductor  $S_1$  is coupled to another superconductor  $S_2$  via a tunnel junction, excess carriers can tunnel through the barrier. At low temperatures ( $T \ll T_c$ , where  $T_c$  is the superconducting critical temperature) recombination time is longer than the tunneling time [2], [4], therefore majority of QPs can tunnel, creating current through a tunnel junction. As the magnitude of current from a detector tunnel junction is inversely proportional to the volume of the source superconductor  $S_1$  [5], in order to enhance the readout signal, Booth proposed the idea of QP trapping in a small volume layer that can be either a superconductor with a smaller gap than that of  $S_1$  or a normal metal [6]. We show a typical quasiparticle trapping device on Fig. 1(a). The current is injected into the device via a tunnel junction from superconductor  $S_{inj}$ , and detected through another tunnel junction with superconducting electrode  $S_2$ .

We have considered a ferromagnetic trap ( $F_{tr}$ ) and investigated the energy confinement produced by downconversion of QPs coming from  $S_1$  into  $F_{tr}$ . *As no gap is induced in  $F_{tr}$  by proximity effect, a ferromagnetic trap allows QPs to relax their energy in a volume much smaller than that of a normal trap, increasing the QP accumulation and hence the local energy density.* We have fabricated three terminal Josephson tunnel devices of different sizes and geometries. QPs are injected into  $S_1$  from a tunnel junction, they relax at the gap edge and then they are trapped in  $F_{tr}$  where through  $e-e$  interaction they locally raise the temperature. The temperature of these nonequilibrium carriers in  $F_{tr}$  is probed by tunneling spectroscopy, measuring the current-voltage characteristics of a second tunnel junction connecting  $F_{tr}$  layer and  $S_2$ . We show that in mesoscopic devices, ferromagnetic trapping is very efficient in raising the local electronic temperature from the bath temperature of 320mK up to 580mK.

The paper is organized as follows. In section II, we describe the principle of quasiparticle trapping. In section III we present the principle of operation of three terminal tunnel junction devices using a ferromagnetic trapping layer. In section IV we describe our three terminal macroscopic device

consisting of two stacked tunnel junctions and present its characterization in terms of conductance variation with QP injection. In section V we present our planar mesoscopic three terminal device, consisting of two tunnel junctions connected with a sub-micrometric S/F bilayer. We also measure conductance as a function of steady-state current injection. In section VI we discuss the results and trap heating in terms of a simple non equilibrium model.

## II. Principle of Quasiparticle Trapping

As first proposed by Booth [6], trapping of excitations in a small junction has been considered as an alternative to fabrication of large area detectors, whose high capacitance limits both the frequency response and the energy resolution. Excess QPs created by either Cooper pair breaking or injection (see Fig.1(a)) diffuse from  $S_1$  to the trap, where they relax their energy and are confined until they recombine into Cooper pairs.

From this intuitive physical picture, it is clear that the trap layer has two crucial functions: it prevents back diffusion of QPs, and with its smaller volume it increases the magnitude of the readout signal, since the density of out of equilibrium quasiparticles  $N^{QP}$ , for a fixed energy, is proportional to the inverse of the trap volume  $N^{QP} = I_{inj} \tau_{tr} / e V_{tr}$ , where  $I_{inj}$  is the injected current,  $V_{tr}$  the trap volume and  $\tau_{tr}$  the time spent in the trap before recombination. However, if the volume is too small, phase coherence is preserved in the trap resulting in a superconducting proximity effect. The induced gap in the density of states in the trap reduces the number of QPs available to relax the energy, and hence heating.

The choice of materials for the Superconductor/Trap ( $S_1/T$ ) bilayer is, therefore, crucial for correct operation. Firstly,  $S_1$  will be chosen for long QP lifetimes and high QP diffusion velocities to ensure that QPs reach the trap before recombination. Secondly, it is important that interfaces between  $S_1$  and T are clean, to facilitate the diffusion. Thirdly and most importantly, we need a small superconducting proximity effect in the trap layer. We should make a trap layer sufficiently thin in order to get a high tunneling rate and density of nonequilibrium QPs, but not too thin as it should remain in the normal state in contact with  $S_1$  through a highly transparent interface. Despite considerable efforts in several laboratories, the right compromise between these constraints is still under investigation.

N.E. Booth et al. [7] and Ullom et al. [8], [9] have extensively studied normal trap efficiency, defined as the ratio between detected and injected power, in a system consisting of an Al superconducting reservoir  $S_1$ , and Ag as the normal metal trap. QPs are injected into a central superconducting Al film using a tunnel junction. The temperature of the Ag electrons is measured by tunneling spectroscopy from the current voltage characteristics of a second junction as shown in Fig.1(a). Tunneling through a detector junction determines the dwell time and the speed of the detector, both of the order of  $\mu s$ . Ullom et al. described the QP diffusion in terms of a renormalized, energy dependent diffusion coefficient  $D_E = (v(E)/v_F) D$ , where  $v(E) = v_F [1 - (\Delta/E)^2]^{1/2}$  is the QP group velocity that drops to zero at the gap edge,  $\Delta$  is the superconducting gap,  $v_F$  the Fermi velocity,  $E$  the energy measured from the Fermi level and  $D$  is the bulk diffusion coefficient. They have measured at 100mK up to 17% efficiency, defined as the ratio between the detected power and the power dissipated by QPs injected at the Al gap edge and relaxing to the Fermi energy in the trap. Because of the large device size ( $\sim 100\mu m$ ), QP losses were mainly due to recombination. In another series of experiments with excitations produced in In crystals by a low power pulsed laser,

Goldie et al. [5] studied trapping into Al and Cu volumes in several devices with different thicknesses (250 to 500nm) and barrier transparencies, always finding a minigap induced in the Cu by the proximity effect. Pepe et al. [10] reported nonequilibrium measurements under steady state current injection in a stacked double superconducting tunnel junction device with middle electrode consisting of an Nb/Al bilayer where the Nb is the superconductor and the Al the trap. They found that the 20nm thick Al trap layer was strongly proximised by a 40nm thick Nb film. They also found that the proximity effect is reduced as a function of the injection current, without any appreciable modification of the interface transparency. Zehnder [11] has studied how external energy is stored for different junction materials. He found losses mainly due to the presence of the sub-gap phonons in the trapping layer that decrease tunneling and hence charge collection. Efficiency scales inversely with the mean free path of the material. He also pointed out that for large area ( $50 \times 50 \mu\text{m}^2$ ) Nb/Al structures the density of states is spatially dependent. As a consequence, the trapping process becomes local, and hence both QP lifetime and trapping rate. To increase the trapping efficiency, Shafranjuk and Nevirkovets [12] proposed a new type of device based on a double Josephson junction in which the middle trapping electrode consists of a thin superconducting layer with a smaller gap compared to the outer electrodes, and which is embedded between two insulating barriers. An Andreev bound state (ABS) level is then formed and characterized by a sharp singularity in the single electron DOS at the gap energy. This resonance is sharper than the BCS gap edge singularity,  $\sim 1/(E^2 - \Delta^2)^{1/2}$ , therefore, it should accumulate a higher number of nonequilibrium QPs than a typical Al trap, leading to increased charge amplification and energy resolution. Moreover, the position of ABS can be tuned by changing the thickness of the superconducting middle layer. So far there hasn't been a report on the experimental realization of this proposal.

In the present work we propose a new direction, the reduction of the trap volume using a ferromagnet  $F_{\text{tr}}$ . While the difference between the energy scales of the superconducting gap and the ferromagnetic exchange energy  $E_{\text{ex}}$  ( $\Delta \sim \text{meV}$ ,  $E_{\text{ex}} \sim \text{eV}$ ) prevents the coexistence of the two states in bulk systems, in nano systems their interaction is limited to the interface. The superconducting proximity effect extends in the ferromagnet over a coherence length given by  $\xi_F = (\hbar D / E_{\text{ex}})^{1/2}$  that varies between 0.1 and 10nm and is almost 100 times smaller than the coherence length of a normal metal with the same diffusion constant,  $D$ . This extremely reduced proximity effect provides a more efficient energy localization. So, a hybrid, mesoscopic S/F heterostructure seems to be a unique candidate to obtain the smallest, not proximised trap.

### III. Three terminal device operation

Here we describe the working principle of our realization of the ferromagnetic quasiparticle trapping transistor (FQTT) based on the description proposed by Booth et al. [13]. Instead of a normal metal, we introduce a weak ferromagnet into the double junction structure: a  $\text{Pd}_{0.9}\text{Ni}_{0.1}$  alloy [14]. This alloy can represent the best choice for a trapping layer because: 1. the small ferromagnetic coherence length ( $\sim 10\text{nm}$ ) leads to smallest trap volumes; 2. Pd has an almost filled  $d$  band, and the large density of states at the Fermi level provides more conduction electrons available in the trap; 3. electronic specific heat is high ( $\sim 3$  orders of magnitude higher than pure Copper, for example) [15], which means that energy is “stored” in the electron gas, with substantially longer  $e$ - $ph$  relaxation time.

The principle of operation of our devices can be obtained considering a simple static balance of power flow into the  $F_{tr}$  layer (Fig. 1(b)). To do this, we borrow the common semiconductor transistor terminology. We call  $S_1/F_{tr}$  bilayer the *base*,  $S_{inj}$  the *emitter*, and  $S_2$  the *collector*. Current  $I_{inj}$  is passed through the first junction emitting  $I_{inj}/e$  QPs. The net power injected into  $S_1$  is  $P_{inj} = (I_{inj}/e) \cdot \epsilon_{inj}$ , where  $\epsilon_{inj}$  is the average injected QP energy, which depends on the voltage  $V$  across the tunnel junction. In our experimental conditions  $\epsilon_{inj} \sim \Delta_{inj}$ , the energy gap of  $S_{inj}$ . Of course, only a fraction of the injected power is collected at the second tunnel junction. Let us assume that the main part of the incoming power is lost via thermal interaction with the phonon lattice,  $P_{th}$ . It can be calculated using the so called 2- $T$  nonequilibrium model [16], in which different temperatures  $T_e$  and  $T_{ph}$  and specific heats  $C_e$  and  $C_{ph}$  are assigned to the electron and phonon systems, which are considered to be decoupled at low temperatures. The energy transfer rate from electrons to phonons in the  $S_1/F_{tr}$  bilayer is given by  $P_{th} = \Sigma V_{tr} (T_e^5 - T_{ph}^5)$ , where  $\Sigma$  is a material-related parameter (varying in the range of  $1\text{-}5\text{ nW}/\mu\text{m}^{-3}\text{K}^{-5}$ ) and  $V_{tr}$  is the volume of the trap. Here we explicitly assume that the phonon system is at the external bath temperature. This hypothesis, as we shall see later, depends on the details of the film geometry and coupling to the substrate, via the Kapitza interface conductance [17]. Injected power is also evacuated via the detector tunnel junction, by cooling through tunnelling. This happens when a NIS junction is biased at a voltage  $V$  lower than the superconducting gap, so that only the hot electrons from the tail of the Fermi distribution can tunnel from the normal to the superconducting electrode. Self cooling, by removing high energy electrons, causes a progressive transfer of energy out of the normal film, which in some cases can reduce its temperature even below that of the substrate [18]. The cooling power of the junction when polarized at the gap edge is given by  $P_{Cool} \approx 0.5 \Delta_2^2/e^2 R_T (k_B T/\Delta_2)^{3/2}$  [19], where  $R_T$  is the normal state resistance of the junction. We emphasize that both the collector voltage ( $V_C$ ) and the current ( $I_C$ ) depend on the increased electronic temperature  $T_e$ .

From power balance we obtain:

$$(I_{inj}/e)\epsilon_{inj} - \Sigma V_{tr} (T_e^5 - T_{ph}^5) \approx 0.5 \Delta_2^2/e^2 R_T (k_B T/\Delta_2)^{3/2}. \quad (1)$$

If the cooling power can be neglected all the injected energy is lost by phonon interactions:

$$(I_{inj}/e)\epsilon_{inj} - \Sigma V_{tr} (T_e^5 - T_{ph}^5) \approx 0,$$

which yields:

$$T_e = T_{ph} [1 + (I_{inj}/e) \cdot \epsilon_{inj} / \Sigma V_{tr} T_{ph}^5]^{1/5}. \quad (2)$$

We stress one crucial aspect of Eq. (2) and its physical meaning. The electron relaxation in a metal depends strongly on the energy of the electronic system. If high energy QPs are injected from the  $S_1$  reservoir into the trap (i.e.  $E_{inj} \gg \Delta_L$ ), the most efficient mechanism for energy redistribution within the electron subsystem becomes the emission of Debye phonons. The mean free path of these phonons is very small, and they efficiently excite additional electrons and break Cooper pairs in the  $S_1$  reservoir. Nonequilibrium vibrations isotropically propagate through the whole system, mixing and coupling the electronic and phononic subsystems. As a result, strong and delocalized heating takes place and energy confinement is no longer possible. It is very important to work at energies near the gap edge in order to avoid phonon losses (which multiply with the increase of the injection energy) and transfer the injected energy solely to the electronic system.

#### IV. Stack junction device

We have fabricated two kinds of three terminal structures with different geometries and sizes. In both we chose Al as superconductor  $S_1$  for its long recombination time [1] (See Eq. (3)).

The first macroscopic device that we shall present consists of two stacked junctions (area of  $0.7 \times 0.7 \text{ mm}^2$ ). We put electric contacts so that we can bias each junction independently. The stacked structures used for the experiment described in the following are sketched in Fig. 2 in a top (a) and side (b) view. Four stacked junctions are fabricated simultaneously on a single Si wafer, with common bottom electrode. All layers were fabricated *in situ* using thin film evaporation, in an ultra high vacuum system with a base pressure of  $10^{-9}$  mbar. The fabrication procedure is as follows. On a Si substrate we evaporated through a metallic mask the first 50nm-thick Al layer. This layer will be the bottom electrode  $S_2$  of the device, common to all the junctions of the sample. Then we oxidize the Al layer by  $\text{O}_2$  plasma at about  $8 \times 10^{-2}$  mbar pressure. The junction area is defined by evaporating 50nm-thick orthogonal striplines of SiO in order to define a square of  $0.7 \times 0.7 \text{ mm}^2$ . Then, a layer of PdNi (10% Ni) is evaporated as ferromagnetic trap  $F_{tr}$ . We have varied the thickness (5, 8, 10nm) of the PdNi layer. The trap volume is  $V_{tr} = 2500 \mu\text{m}^3$  for 5nm of PdNi. Then we evaporated 250nm of Al as superconducting layer  $S_1$ . Then we repeated the oxidation and SiO deposition in order to make a second tunnel barrier, and finally evaporated 50nm of Al as layer  $S_{inj}$ . The junctions quality was systematically checked by measuring the current-voltage characteristics and the tunnel conductance with the standard ac modulation technique. All the measurements were carried out at 320mK in a  $^3\text{He}$  cryostat. In Fig.3 are shown two typical  $I$ - $V$  curves and tunnel conductance spectra of an Al/ $\text{Al}_2\text{O}_3$ /Al (SIS) junction (a) and an Al/ $\text{Al}_2\text{O}_3$ /PdNi-Al (SIF) junction (b). Quasiparticle current is suppressed below  $360 \mu\text{V}$ , i.e. twice the Al gap for the upper SIS junction, while for the bottom SIF junction we measure a voltage gap of  $195 \mu\text{V}$  showing no proximity effect in F. The tunnelling spectrum of the bottom junction is well fitted by the conventional BCS density of states (dotted line). Normal resistances are  $140 \Omega$  for SIS and  $4 \Omega$  for SIF junction. The critical temperature of the PdNi/Al bilayer is 1.2K.

We measured the dynamical conductances of the bottom and top junction under injection of current between 0 and  $600 \mu\text{A}$ . These current values correspond to injected QP energy between  $\Delta_{Al}$  ( $I_{inj}=3 \mu\text{A}$ ) and  $45\Delta_{Al}$  ( $I_{inj}=150 \mu\text{A}$ ). We did not observe any enhancement in the detection spectra at energies close to the gap, while at energies 50 or even 100 times larger, zero bias conductance increases linearly in power (variations of about 10% are measured) due to hot electrons. We have also reversed the roles of the junctions and injected QPs at energies varying from  $1.85\Delta_{Al}$  to  $10\Delta_{Al}$ , but observe no enhancement in the detection spectra in this configuration. The injected power is of the order of  $\mu\text{W}$  in both configurations. As shown in Fig. 4, curves (1) and (2) refer to the injection and detection in the same stack. Blue curve (1) corresponds to injection from the SIF and detection at the SIS and red curve (2) to the inverse. For the injected power where phonon emission drives the relaxation process, we measure twice higher signal when injecting from the SIF (1) rather than the SIS (2) junction because of the double convolution by the QP density of states of the two superconducting reservoirs in the calculation of conductance.

Curves (3) refer to injection and detection between junctions of different stacks. All curves (3) are practically superimposed, regardless of the direction of injection. No differences are observed in the detector as a function of the distance from the injector. Therefore even though energy is not localized in  $F_{tr}$ , the lack of accumulation is not due to the out diffusion of the QPs away from the detector junction area into the surroundings. Quasiparticles basically stay and eventually recombine where they have been injected. Indeed, from the recombination time  $\tau_r = 100 \mu\text{s}$  which sets the upper

limit for QP diffusion, we found diffusion length  $L_r \sim 10\mu\text{m}$ , which is small compared to the dimensions of our device. We remind that  $\tau_r$  is given by

$$\tau_r^{-1} \cong \tau_0^{-1} \sqrt{\pi \left( \frac{2\Delta}{k_B T_c} \right)^5} \sqrt{\frac{T}{T_c}} \exp\left(-\frac{\Delta}{k_B T}\right), \quad (3)$$

where  $\tau_0$  is the Kaplan timescale parameter ( $\sim 0.5\mu\text{s}$  for the Al),  $\Delta$  and  $T_c$  the gap and critical temperature of Al. Moreover, we did not register any difference between the injection from the top/bottom junction of the stack and detection with the bottom junction of the neighbouring stack. This implies, as the bottom electrode is geometrically common to all the junctions of the sample, that the tiny raise in the tunnelling conductance (i.e. curve (3)) is mainly due to the phonon bath (we also did not measured any thermal gradient between neighbouring junctions). Let us consider the power balance and the dynamics of excitations in the PdNi trap. We calculate specific heat of electron and phonon subsystems:  $C$  (mJ/mol·K) =  $\gamma T + \beta T^3$ , where the linear contribution is due to electrons and cubic to phonons. From the molar volume of the trap ( $8.64\text{cm}^3/\text{mol}$ ) we have:  $\gamma_M = 1.38 \times 10^{-15} \text{J} \cdot \mu\text{m}^{-3} \text{K}^{-2}$  and  $\beta_M = 1.7 \times 10^{-17} \text{J} \cdot \mu\text{m}^{-3} \text{K}^{-4}$  and hence:  $C_e = 1.0 \times 10^{-12} \text{J/K}$  while  $C_{ph} = 1.2 \times 10^{-15} \text{J/K}$  at 300mK. We found that the electron-phonon conductance ( $dP_{ph}/dT_e \equiv G_{e-ph} \approx 5 \Sigma (Ad) T_e^4$ ) at  $T_e = 300\text{mK}$  is  $0.2\mu\text{W/K}$  and the electron-phonon scattering time ( $\tau_{e-ph} = C_e / G_{e-ph}$ ) is  $5.1\mu\text{s}$ . Once thermal excitation is transferred to the lattice, energy can flow by thermal conductance to the substrate. This transfer is limited by thermal boundary resistance, the Kapitza resistance,  $R_K$ . Typically,  $R_K \cdot T^3 = 5 \times 10^{-4} \text{K}^4 \text{m}^2 \text{W}^{-1}$ . Thus the effective conductance will be:

$$G_K = \frac{\text{Area}}{R_K} = \frac{T^3}{5 \times 10^{-4}} \left[ \frac{\text{Area}}{1 \text{m}^2} \right] \text{W/K}.$$

There are two boundaries to consider: PdNi to Al bottom electrode, and bottom electrode to substrate. We neglect the boundary between the surface oxide on the substrate and the single crystal Si wafer. So, taking as area a larger value of about  $1\text{mm}^2$  and considering the series of two interfaces, we obtain  $G_K = 27\mu\text{W/K}$ , which implies  $G_K$  about a factor 100 larger than  $G_{e-ph}$ . The phonon temperature is uniform on the sample. This implies that our substrate has very good coupling to the  $\text{S}_1/\text{F}_{tr}$  bilayer, which is consistent with a very high Kapitza interface conductance.

We now discuss why the ferromagnetic trap is not working properly. The trap works at the gap edge and, in our case, at that energy the flow of injected QPs is too small. To fulfill the first condition we need the density of out of equilibrium QPs in the trap to be higher than that in the thermal equilibrium,  $N^{QP} > N_0^{QP}$ . This condition imposes a lower bound on the lifetime of the out of equilibrium excitations in the trap  $\tau_{tr}$  as  $N^{QP} = I_{inj} \tau_{tr} / e V_{tr}$  and  $N_0^{QP} = n(\epsilon_f) k_B T$ , where  $I_{inj}$  is the injected current (typically of about  $1\mu\text{A}$  at the gap edge with our resistance values),  $V_{tr}$  is the trap volume, and  $n(\epsilon_f)$  is the density of electron states at the Fermi level. We estimated that  $\tau_{tr}$  of about  $300\mu\text{s}$  is required to accumulate excitations with a number higher than  $N_0^{QP}$ . This time is much larger than any characteristic timescale and in particular  $\tau_{e-ph}$ , thus excitations out of equilibrium created by injection are practically lost via phonon interactions. The trap is inefficient and the conductance at zero bias independent of injection at energy comparable with the Al gap edge.

The first obvious solution is to increase the injected current density.

## V. Mesoscopic planar device

We fabricate a new type of mesoscopic planar device to get smaller volumes and higher trap efficiency. This type of device is represented in the photo of Fig.5(b). Two sub-micrometric tunnel junctions are separated by middle, double layered Al-PdNi common electrode, the trap. The Al superconductivity is strongly suppressed due to the large inverse proximity effect.

The fabrication is as follows. We used a trilayer suspended mask consisting of 600nm of polymer polyether sulphone (PES), 60nm  $\text{Si}_3\text{N}_4$  layer, and 400nm PMMA layer. The mask is patterned by electron beam lithography and the pattern transferred to the  $\text{Si}_3\text{N}_4$  layer by  $\text{SF}_6$  plasma reactive ion etching at a pressure of 10mbar for about 60 seconds. Then the PES is etched with  $\text{O}_2$  plasma at a pressure of 300mbar for 10 minutes, which gives an undercut of about 500nm. The SEM photo of the mask is shown on Fig. 5(a). Our samples were fabricated by angle evaporation in an ultrahigh vacuum system with a base pressure of about  $10^{-8}$ mbar. First 50nm of Al were evaporated. The Al was oxidized in pure  $\text{O}_2$  flux at a pressure of  $5 \times 10^{-2}$ mbar. Then a 50nm-thick Al layer was evaporated, followed by a 5nm-thick PdNi layer. Four devices are fabricated on the same wafer. The SEM image of the device is shown in Fig. 5(b). The first, right-side  $300 \times 500 \text{ nm}^2$  Al/ $\text{Al}_2\text{O}_3$ /Al junction is separated by another junction of the same area by a  $4 \mu\text{m}$  long Al layer which is partially ( $\sim 3 \mu\text{m}$ ) recovered by a thinner ferromagnetic PdNi layer. The magnetic layer is used to suppress superconductivity by inverse proximity effect and it defines the trap. Trap volume is  $V_{tr} = 0.15 \mu\text{m}^3$  i.e. about 100 times smaller than the trap used in the stacks.

Note that the F layer plays a slightly different role in this device, since the QPs coming from the Al superconducting reservoir go through a tunnel barrier into the bilayer made up of the same superconductor. As the reservoir and the trap are made of the same material, matching of the Fermi velocities is optimal and so is the QP transmission. In this planar structure we deal with lateral trapping, which allows to avoid back tunnelling of QPs, responsible for reduced cooling power [19], [20].

In Fig. 6, the I-V curves of the Al/ $\text{Al}_2\text{O}_3$ /Al (SIS) and the Al/ $\text{Al}_2\text{O}_3$ /Al/PdNi (SI/SF) junctions are shown. The normal state resistances are about  $750 \Omega$  and  $500 \Omega$ , respectively. Junction resistances higher than those measured in the stacks result in reduced injected power (now ranging from 50pW to 1nW). The gap voltages are  $400 \mu\text{V}$  and  $200 \mu\text{V}$ , as expected for inverse proximity effect. Moreover, the I-V curve of the SI/SF junction is well fitted by integrating the BCS density of states with an Al energy gap of  $190 \mu\text{eV}$  and a base temperature of 320mK (see Fig.7). The SIS junction is hysteretic with critical current of 200nA and retrapping current of 85nA. The finite resistance at zero bias is due to the bilayer trap resistance in series with the junction. The principle of the experiment is the same as that described above. Current injection creates out of equilibrium excitations. These excitations are collected in the SF trap rising the electron temperature,  $T_e$ , which is measured by tunnelling spectroscopy. Different conductance spectra were measured, while increasing the DC injection current through the SIS junction from 0.3 to  $8 \mu\text{A}$ , as shown in Fig. 7. We obtain  $T_e$  from the BCS fits also shown in Fig. 7 as red curves. The electron temperature  $T_e$  as a function of the injected current is plotted in Fig. 8, top panel, markers. The temperature rises rapidly up to 0.53K, and then reaches 0.98K more slowly, resulting in two different slopes. Unlike stack junctions, the temperature in the planar trap increases significantly for the injection of QPs with energy comparable with the superconducting gap energy. Furthermore, the crossover between these two regimes is set by a voltage bias corresponding to the gap edge as expected because trapping, and hence energy localization, are efficient only below the gap edge. As injection energy increases ( $\sim 40$  times more for  $I_{inj} = 8 \mu\text{A}$ ) out of equilibrium phonons are emitted before the QPs reach the trap.

High energy relaxation occurs mainly by phonons, therefore energy is not localized in the trap, resulting in a smaller temperature increase.

## VI. Trap heating

Quasiparticles injected below the gap edge enter into the trap where they relax their energy  $\Delta_{inj}$ . This is possible because, firstly, at 0.3K the trap size is larger than  $L_{ee} = (D \cdot \tau_{ee})^{1/2} = 3\mu\text{m}$ , secondly, the electron-phonon scattering time is much longer than  $\tau_{ee} \sim 10\text{ns}$  and thirdly, the trap is located at a distance of about a micrometer from the SIS junction. This distance is much smaller than the recombination length  $L_r \sim 100\mu\text{m}$  as estimated above. An estimation of the electron-phonon scattering time from the electron-phonon conductance  $G_{e-ph} = 1.6\text{pW/K}$  and the specific heat  $C_e = 6 \times 10^{-15}\text{J/K}$  gives  $\tau_{e-ph} = 0.5\mu\text{s}$ . The effective surface trap area evaluated from the SEM image is about  $3\mu\text{m}^2$  and it gives  $G_K = 160\text{pW/K}$  Kapitza conductance from the phonon bath to the substrate. As  $G_K \gg G_{e-ph}$ , the phonons in the device are thermalized at the phonon base temperature. Finally, we computed the thermal tunnelling conductance using the approximate formula [13]:

$$G_C \approx \varphi(1/2 + \varphi)k_B I_C / e, \text{ where } \varphi = \frac{(A_2 - eV_C)}{k_B T_e}.$$

The tunnelling time is given by  $\tau_t = C_e / G_C$ . At a voltage near the gap edge ( $V=170\mu\text{V}$ ) and  $T=0.3\text{K}$  we found:  $G_C = 10\text{pW/K}$  and  $\tau_t = 70\text{ns}$ . The bandwidth of the device is limited by the smallest between thermal tunnelling and electron-phonon time [13]. In Table I are summarized all the relevant physical parameters that determine QP trapping, for both stacks and mesoscopic devices investigated here.

In Fig.8 (top panel, full line) we report the temperature increase as estimated from Eq. (2) considering negligible cooling by tunnelling. (An estimate gives about 2pW, a factor hundred smaller than the injected power.) The actual temperature increase is lower than that obtained considering only cooling by phonons. Instead, we found good agreement by introducing a QP thermal loss (dotted-dashed line),  $\kappa \cdot \Delta T$ , where  $\kappa$  is the thermal conductivity of the Al leads whose normal state resistance is  $1.2\Omega$ .

Now let us discuss the current gain. The excess current of the SI/SF junction normalized to the value for zero injected current,  $\Delta I_C / I(0)$ , for three different voltage bias values, is shown in Fig. 8, bottom panel. When biasing well above the gap voltage (curve C on Fig. 8 corresponding to point C on Fig. 6,  $V_C = 0.28\text{mV}$ ), no excess current is measured. This range corresponds to the *high energy tails* of the QP DOS and it is almost independent of injection. When we approach the gap voltage we measure more pronounced variations of the collected current. When we polarize the detector junction at  $V_C = 0.1\text{mV}$  (i.e. below the gap voltage, point A on Fig. 6) we measure an increase of the tunnel current up to 15 times. As expected, it is at energies near the gap that the increase of current is maximum: at  $V_C = 0.18\text{mV}$ , point B on Fig. 6, the collected current is up to 35 times  $I_C(0)$ . It is important to note that the trapping mechanism not only controls the number of out of equilibrium QPs, but also the direction of the energy flow. If we reverse the roles of the junctions, injecting from the SI/SF and detecting at the SIS, we do not register any increase of output current.

All the current values detected in the reversed configuration fall below the dashed line in Fig. 8, low panel. Therefore, the ferromagnetic trap introduces a strong asymmetry in the device. This property is very interesting for possible applications as a three-terminal, transistor-like device. However the amplification parameter as defined by Booth [13],  $\beta = I_C / I_{inj}$ , where  $I_C$  and  $I_{inj}$  are, respectively, the

collected and injected currents, normalized to the current gap values  $I_{C0}=I_{inj0}=\Delta_{Al}/R_N$ , is 0.24 for detection at constant normalized voltage  $V_C=0.8$ . Higher amplification may be achieved at lower temperature and highly thermally isolated traps.

## VII. Conclusion

We have investigated a three terminal device consisting of two superconducting tunnel junctions coupled via an S/F bilayer. The ferromagnetic layer is used to localize and multiply QPs injected from the base junction. QP excess current is measured through the second detecting tunnel junction. We measured conductance spectra of the detecting junction as a function of the injected power for two types of structures fabricated with the same S/F materials: a stacked macroscopic and a planar mesoscopic device. We have found efficient trapping in the mesoscopic device, where it is possible to increase the local electronic temperature by up to 60% of the base temperature. We have also found that input is well isolated from the output as a consequence of using the ferromagnetic trap, making the device attractive for transistor-like operation. However the gain at 320mK is 0.24.

## VIII. Acknowledgments

This work was partially done at the Quantum Physics Laboratory at the ESPCI and it was supported by the ESPCI and the ESF through the “Pi-Shift” project. J. Lesueur, B. Leridon, B. Reulet, G.P. Pepe and A. Barone are gratefully acknowledged for several ideas and discussions. We also thank S. Collin for technical assistance.

## References

- [1] S. B. Kaplan, C.C. Chi, D.N. Langenberg, J.J. Chang, S. Jafarey and D. J. Scalapino, Phys. Rev. B **14**, 4854 (1976).
- [2] R.Cristiano in “*Superconducting detectors*”, Proceedings of 5<sup>th</sup> SceNet School, Spain, Sept. (2004).
- [3] A. Zehnder, Phys. Rev. B **52**, 12858 (1995).
- [4] *Nonequilibrium Superconductivity, Phonons, and Kapitza Boundaries*, edited by K. E. Gray (Plenum, New York, (1981).
- [5] D. J. Goldie, N. E. Booth, C. Patel and G.L. Salmon, Phys. Rev. Lett. **64**, 954 (1990).
- [6] N. E. Booth, Appl. Phys. Lett. **50**, 293 (1987).
- [7] J. N. Ullom, P. A. Fisher and M. Nahum, Nucl. Instr. and Meth. A **370**, 98 (1996).
- [8] J. N. Ullom, P. A. Fisher and M. Nahum, Phys. Rev. B **58**, 8225 (1998).
- [9] J. N. Ullom, P. A. Fisher and M. Nahum, Phys. Rev. B **61**, 14839 (2000).
- [10] G. P. Pepe, G. Peluso, R. Scaldaferrì, A. Barone, L. Parlato, R. Latempa, and A. A. Golubov, Phys. Rev. B **66**, 174509 (2002).
- [11] A. Zehnder, Ph. Lerch, S. P. Zhao, T. Nussbaumer, E. C. Kirk and H.R. Ott, Phys. Rev. B **59**, 8875 (1999).
- [12] S. E. Shafranjuk and I. P. Nevirkovets, IEEE Trans. on Appl. Sup. **15**, 1051 (2005).
- [13] N. E. Booth, P. A. Fisher, M. Nahum and J. N. Ullom, Supercond. Sci. Technol. **12**, 538 (1999).
- [14] A.W. Overhauser and A.I. Schindler, J. Appl. Phys. **28**, 544 (1957).
- [15] G. Chouteau, R. Fourneaux, R. Tournier and P. Lederer, Phys. Rev. Lett. **21**, 1082 (1968).
- [16] V.E. Gusev and O.B. Wrigth, Phys. Rev. B **57**, 2878 (1998).
- [17] E.T. Swartz and R.O. Pohl, Rev. Mod. Phys. **61**, 605 (1989).
- [18] F. Giazotto, T. T. Heikkilä, A. Luukanen, A. M. Savin and J. P. Pekola, cond-mat/0508093 v4.
- [19] K. Segall, C. Wilson, L. Li, L. Frunzio, S. Friedrich, M. C. Gaidis and D. E. Prober, Phys. Rev. B **70**, 214520 (2004).
- [20] J. Jochum, C. Mears, S. Golwala, B. Sadoulet, J. P. Castle, M. F. Cunningham, O. B. Drury, M. Frank, S. E. Labov, F. P. Lipschultz, H. Netel, and B. Neuhauser, J. Appl. Phys. **83**, 3217 (1998).

TABLE I.

<b>Device</b>	<b>Macroscopic stacked</b>	<b>Mesoscopic planar</b>
Trap volume (cm <sup>3</sup> )	10 <sup>-9</sup>	10 <sup>-13</sup>
$G_{e-ph}$ (nW/K)	200	0.02
$\tau_{e-ph}$ ( $\mu$ s)	5	0.5
$G_C$ (nW/K)	2.2	0.01
$\tau_t$ ( $\mu$ s)	700	0.07
Injected power (nW)	1000	1

FIG. 1

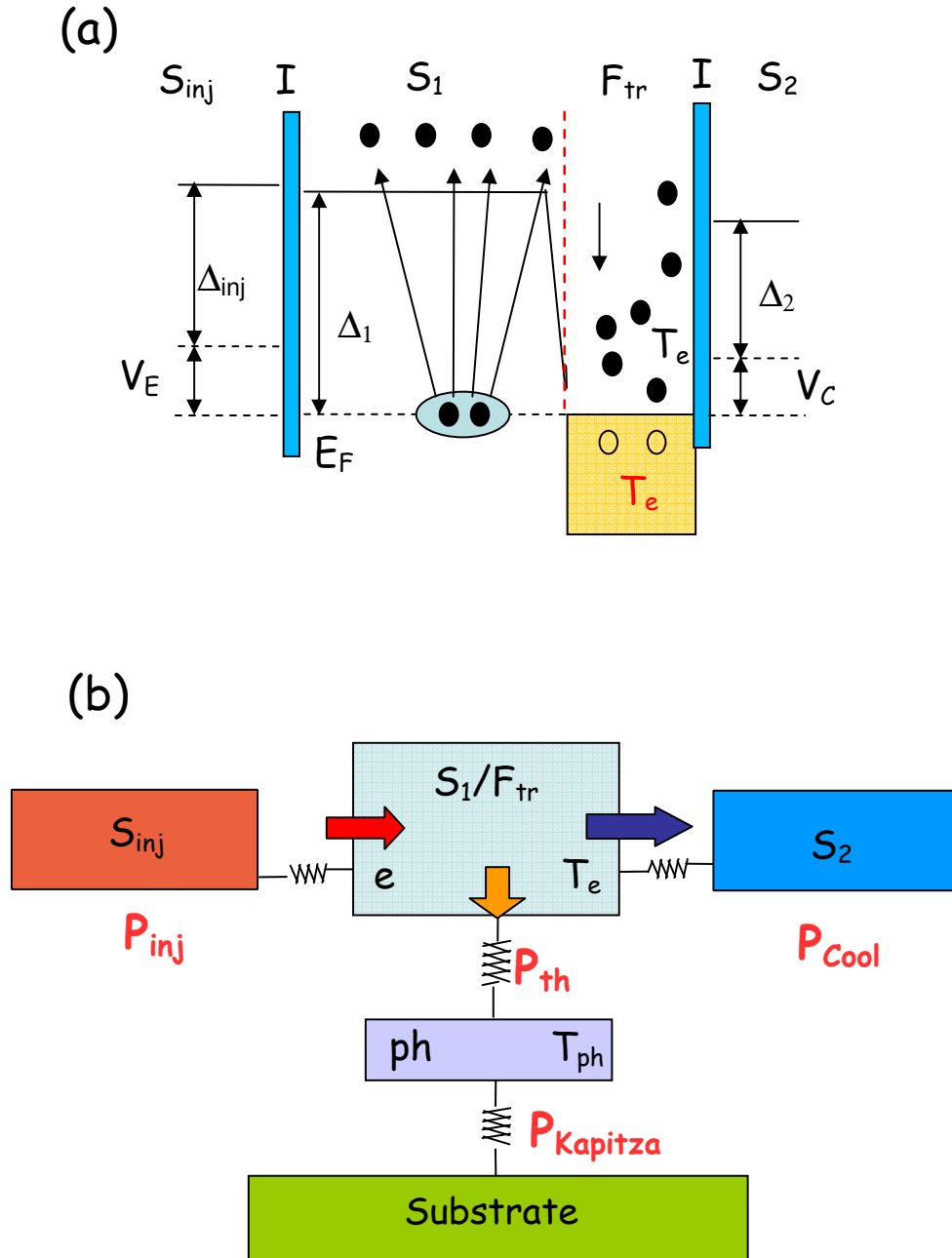


FIG. 2

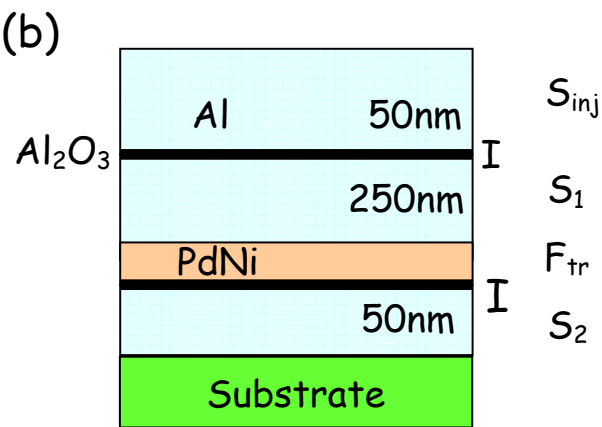
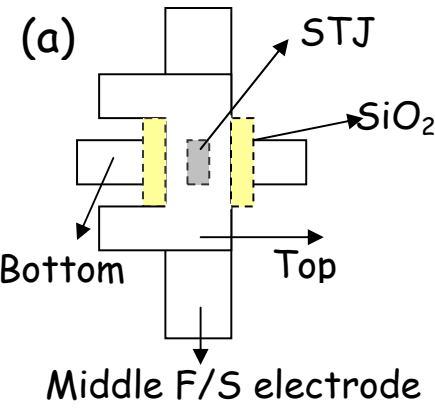


FIG. 3

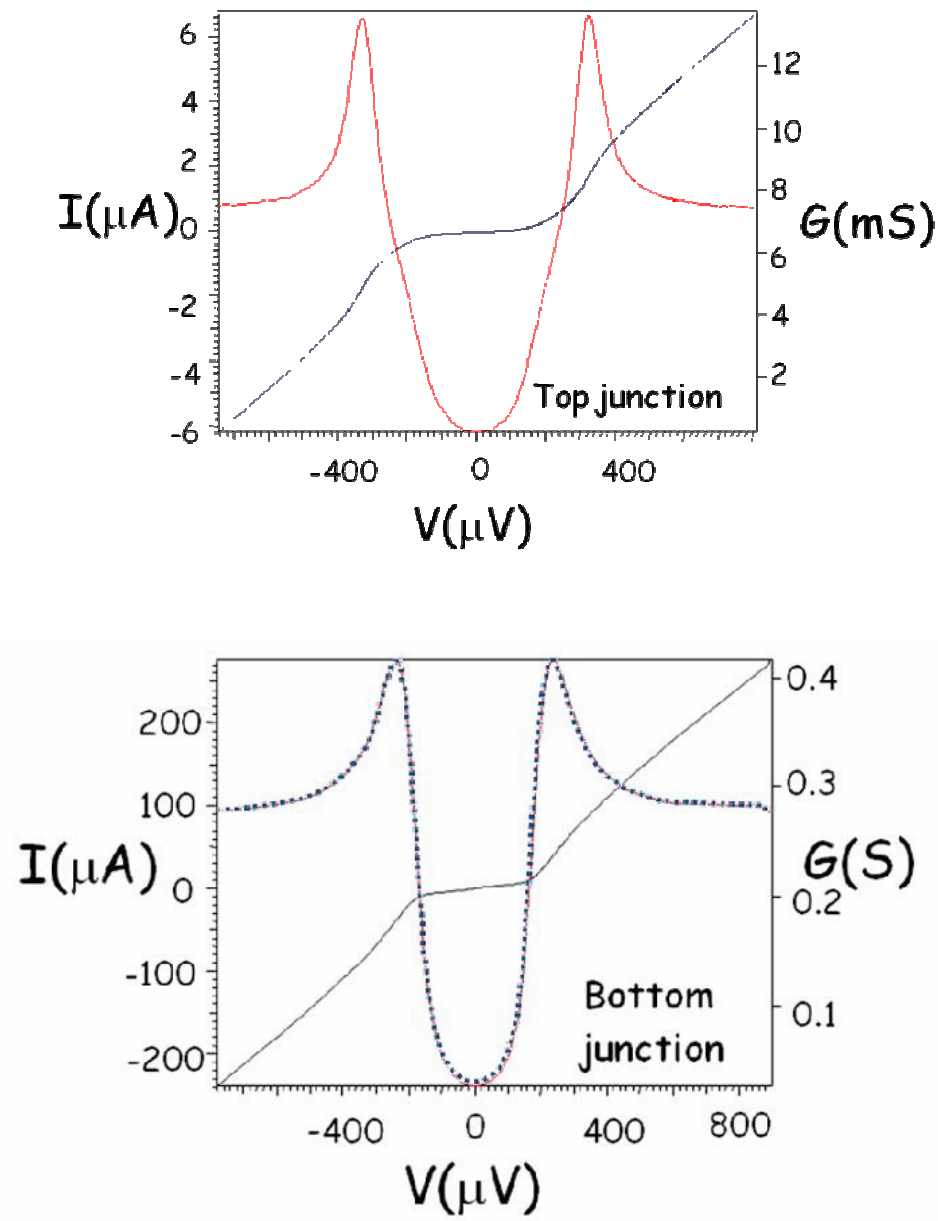


FIG. 4

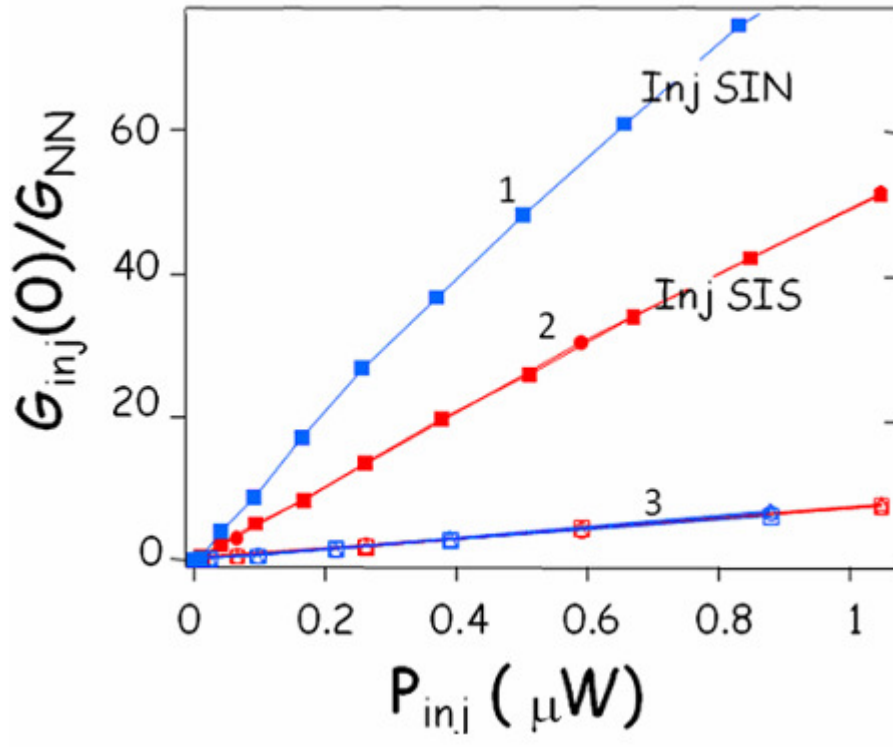


FIG. 5

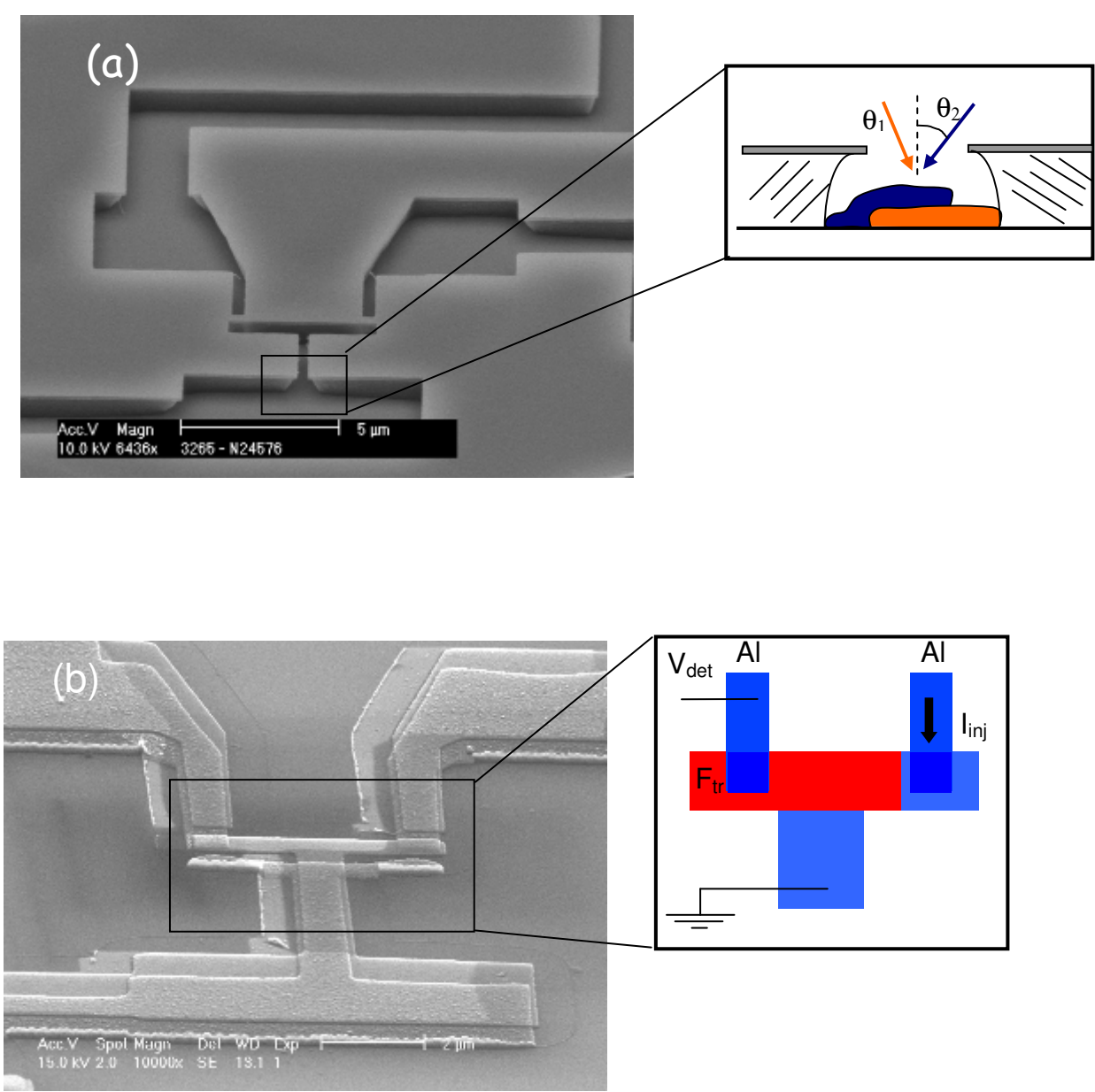


FIG. 6

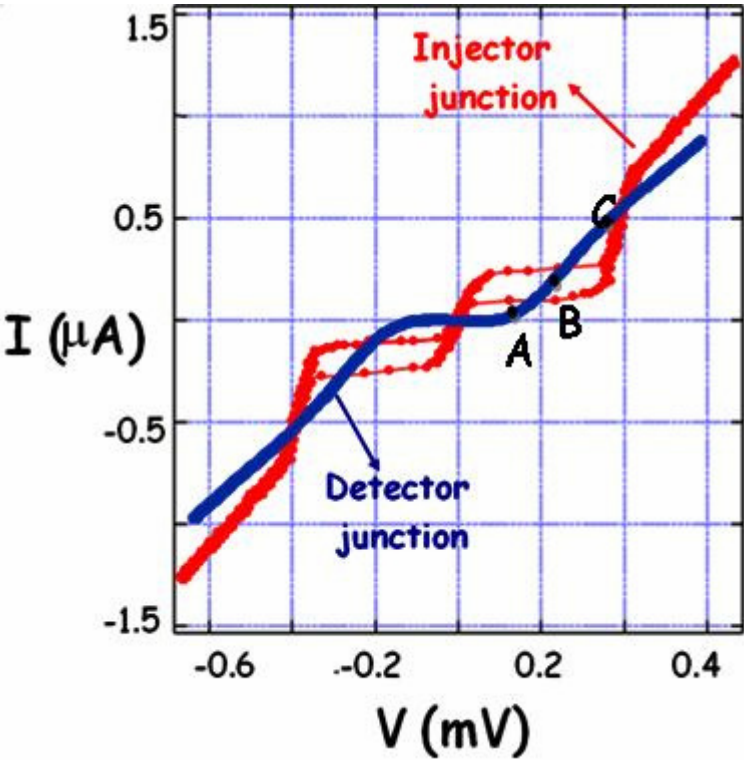


FIG. 7

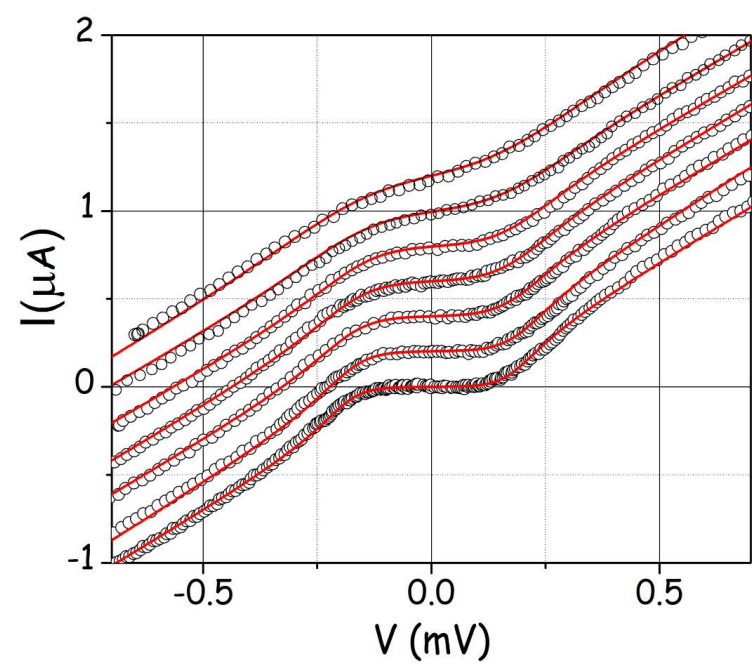
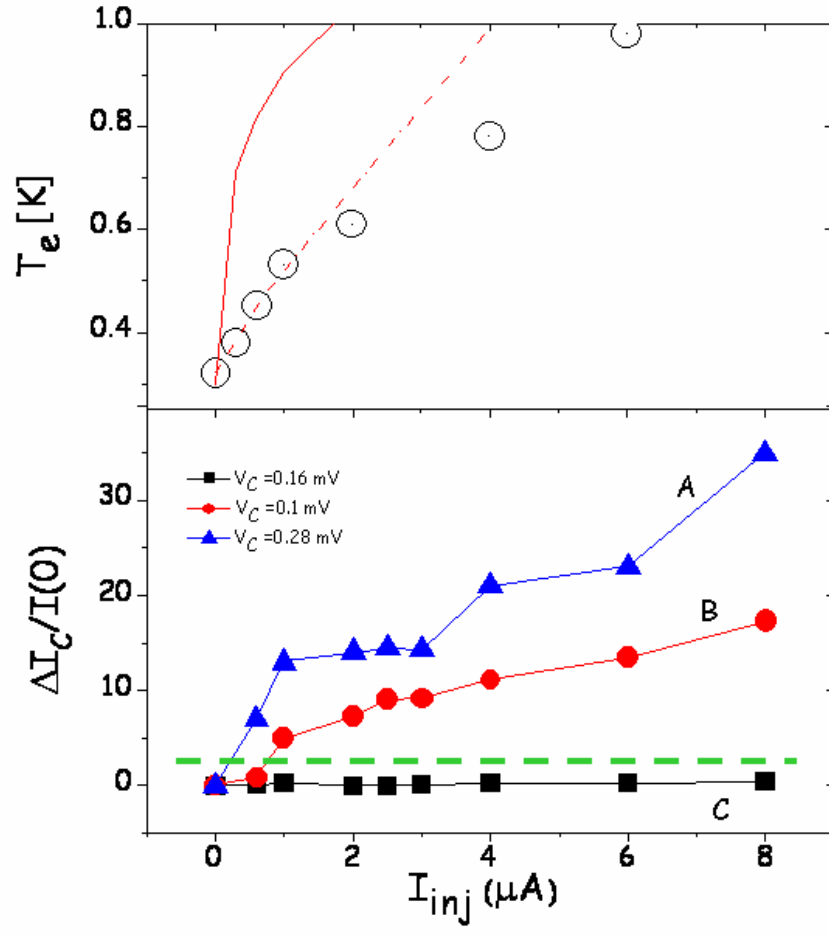


FIG. 8



## Captions

**TABLE I.** The physical parameters which determine the QP dynamics in both traps are summarized. First column refers to the stacked macroscopic devices, and the second to the planar mesoscopic structures.

**FIG. 1 (a)** Principle of quasiparticle trapping. Quasiparticles coming from superconducting reservoir  $S_1$  with energy comparable to the gap fall into the potential well  $F_{tr}$ , and interact with the electrons heating them. A tunnel barrier  $I$  in direct contact with the trap electrode allows the readout of the nonequilibrium current signal. Principle of measurement in is also shown. Electrical access to the three electrodes allows to bias the two junctions in different configurations.

**(b)** Power balance in the trap. The injected power  $P_{inj}$  is partially converted into cooling power,  $P_{Cool}$  (“hot” electrons are removed by tunnelling into the superconducting electrode  $S_2$ ), and lost via phonon interactions in the trap,  $P_{th}$ , and across the surface towards the substrate,  $P_{Kapitza}$ . From power balance, the basic equation which rules the operation of the device is deduced.

**FIG. 2** Sketch of the top view **(a)** and the cross-section **(b)** of the stacked device. Junction area is  $0.7 \times 0.7 \text{ mm}^2$  and distance between junctions on the same sample is about  $1 \text{ mm}$ .

**FIG. 3** Experimental I-V curves and conductance spectra of the top (top panel) SIS and bottom (bottom panel) SIF junction of the stacked device. Normal resistances are, respectively,  $140$  and  $4\Omega$ . In the bottom panel the BCS fit (dotted line) of the conductance spectrum at  $T=0.32K$  and gap value of  $0.195 \text{ meV}$  is also shown.

**FIG. 4** Tunnelling conductance variation at zero bias (normalized to the normal state conductance) as a function of the injected power. Curves (1) and (2) refer to the injection and detection in the same stack. Curve (1) corresponds to the injection from the SIF and detection at the SIS and curve (2) vice versa. Curves (3) refer to the injection and detection between junctions of different stacks.

**FIG. 5 (a)** SEM image of the trilayer mask. In the inset is shown an example of angle evaporation. **(b)** SEM image of the planar device. The Al/AlO/Al junction on the right and Al/AlO/Al/PdNi junction on the left are shown in the inset. They are connected by a  $1\mu\text{m}$  wide Al/PdNi bilayer. In the inset the schematic of the measuring setup is also shown. DC currents are injected from the right SIS and detected through the SIF junction.

**FIG. 6** I-V curves of the Al/AlO/Al junction (red) and the Al/AlO/Al/PdNi junction (blue). On the current voltage characteristics of the Al/PdNi curve are marked three points (A, B, C) which identify three different values of the detection polarization.

**FIG. 7** Experimental I-V curves (dots) and BCS fits (red lines) of the detector junction under a DC current injection between  $0.3\mu\text{A}$  and  $8\mu\text{A}$ .

**FIG. 8 (Top panel)** Electronic temperature in the trap, as a function of the injected current. Markers refer to electronic temperature extracted by experimental conductance spectra via BCS fit. Change in the slope occurs approximately at  $0.75\mu\text{A}$ , corresponding to the Al gap. The full line represents the expected increased temperature, calculated by the electron - phonon coupling. The

dotted-dashed line corresponds to the increase of the electronic temperature due to Al QP thermal conductivity.

**(Bottom panel)** Extra-currents (i.e. difference between detected currents with and without injection, normalized to their value without injection:  $\Delta I_C/I_C(0)$ ) at three different polarizations. (**A**, **B**, **C** points are given in Fig. 6) as a function of the injected current.